

# Shock-Tube CO Measurements during the Combustion of Ethylene Carbonate, a Battery Electrolyte Component

Claire M. Grégoire<sup>1</sup>, Eric L. Petersen<sup>1</sup>, Olivier Mathieu<sup>1</sup>,  
Keisuke Kanayama<sup>2</sup>, Hisashi Nakamura<sup>2</sup>, Kaoru Maruta<sup>2</sup>

1: J. Mike Walker '66 Department of Mechanical Engineering, Texas A&M University  
College Station, Texas, USA

2: Institute of Fluid Science, Tohoku University, 2-1-1 Katahira, Aoba-ku, Sendai 980-8577,  
Japan

## 1 Introduction

One of the major components of commercial lithium-ion batteries is ethylene carbonate (EC), a critical electrolyte which facilitates the dissociation of lithium salts and prevents solvents from decomposing on the graphite anode [1]. With the increase in the market share of electric vehicles, reports of battery fire events after a collision or due to a conception default are more and more frequent. Therefore, a good understanding of EC pyrolysis decomposition and combustion characteristics is of interest to find suitable thermal management strategies and/or suitable fire suppressants. Both directions will ensure a higher safety level for this flammable electrolyte, making it desirable for the next-generation LIBs with competitive performance. The chemical structure of the cyclic EC is shown in Fig. 1 for reference.

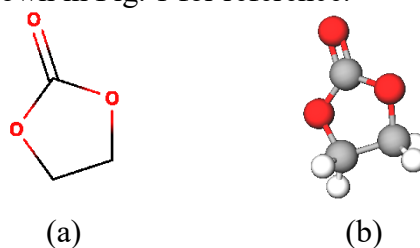


Figure 1: Chemical structure for Ethylene Carbonate (EC) in a) 2D, and b) 3D.

To the best of the authors' knowledge, the experimental database for the EC is extremely limited, with only the study from Kanayama *et al.* where these authors performed an experimental and modeling study on the EC pyrolysis diluted in DMC [1]. The DMC was used as a solvent because the EC is in a solid state at room temperature/atmospheric pressure. Results were obtained in a micro-flow reactor with a controlled temperature profile with species measurements. The experimental details of this study are reported in Table 1. As one can see, new experimental measurements of EC are necessary to extend the current database and further validate the model. Thus, EC high-temperature chemistry was examined by measuring CO time histories using laser

absorption diagnostic in a shock tube, in pyrolysis conditions and for three equivalence ratios ( $\phi = 0.5, 1.0, \text{ and } 2.0$ ), near atmospheric pressure. This work is organized as follows: the experimental method and our conditions are introduced. Then, the new pyrolysis and oxidation results are presented. Finally, chemical kinetics analyses are shown in the discussion section.

Table 1: Summary of the measurements from the literature performed for EC. TOF-MS stands for Time-of-flight mass spectroscopy and GC stands for gas chromatography.

Study	Experimental Conditions
Kanayama <i>et al.</i> [1]	Micro-Flow Reactor: Speciation at 1 atm Mixture: 0.112%EC/0.088%DMC/N <sub>2</sub>  TOF-MS and GC quantification: EC, DMC, H <sub>2</sub> , CO, CO <sub>2</sub> , CH <sub>4</sub> , C <sub>2</sub> H <sub>2</sub> , C <sub>2</sub> H <sub>4</sub> , and C <sub>2</sub> H <sub>6</sub> with $T_{w,max} = 700 - 1200$ K  GC quantification: DME with $T_{w,max} = 900 - 1200$ K GC identification: CH <sub>3</sub> CHO, CH <sub>2</sub> O with $T_{w,max} = 900 - 1200$ K

## 2 Experimental Method

### a Shock Tube and Experimental Conditions

Experiments were conducted in the stainless-steel High Pressure Shock Tube at Texas A&M University, suited specifically for chemical kinetics measurements. The driver and driven sections have dimensions of 2.42-m long, 7.62-cm inner diameter, and 4.72-m-long, 15.24-cm inner diameter, respectively, and are separated by a 0.25-mm thick-film polycarbonate-material. A single diaphragm was used, and a cross-shaped cutter was mounted to allow for consistent diaphragm breakage. The incident shock-wave velocity is obtained by recording the passage of the shock using four PCB P113A piezoelectric pressure transducers placed on the last 2 m of the driven section sidewall. The normal-shock equations give the final temperatures and pressures,  $T_5$  and  $P_5$ , respectively. To maintain high purity for chemical kinetics experiments, a vacuum system utilizing a turbomolecular pump is used to achieve pressures of  $10^{-5}$  torr or better prior to each test. More details on the shock tube can be found in Mathieu *et al.* [2].

The pyrolysis and oxidation of EC in He/Ar was carried out in this shock tube which was heated to a uniform temperature of 100°C using a custom-made heating jacket composed of five independently controlled elements. Additional heating elements and fiberglass insulation set at 120°C were applied to the mixing tank and manifold to prevent any possible fuel condensation during the mixture preparation, where higher pressures of fuels were used. It is worth mentioning that EC is in a solid state at room temperature/atmospheric pressure and has a low vapor pressure even at 120°C according to our observations. The temperatures and pressures used to prepare the highly diluted mixtures of this study ensure the vaporization of EC well below the maximum EC pressure observed in our conditions: 1.57 torr maximum was used to prepare the mixtures, and a vapor pressure of up to about 7.5 torr at 120°C was observed. It should be noted that our observation cannot be considered a vapor pressure measurement at 120°C, and no attempt was made to measure this parameter. Finally, the experimental results were obtained for temperatures ranging from 1212 to 1734 K, and pressures ranging from 1.14 to 1.35 atm. Table 2 reports the

experimental conditions covered during this study. The solid EC came from Sigma Aldrich with a purity of 98%, and the gases O<sub>2</sub>, He, and Ar were provided by Praxair, all with 99.999% purity. EC was degassed several times before its introduction in the mixing tank.

Table 2: Experimental conditions covered during this study.

$\phi$	$X_{EC}$	$X_{O_2}$	$X_{He}$	$X_{Ar}$	Temperature (K)	Pressure (atm)
0.5	0.0005	0.0025	0.2	0.797	1284 - 1695	0.98 - 1.11
1.0	0.0009	0.0021	0.1995	0.7975	1345 - 1717	1.02 - 1.06
2.0	0.0013	0.0017	0.2015	0.7955	1303 - 1704	1.01 - 1.10
$\infty$	0.001	0	0.2	0.799	1304 - 1736	1.02 - 1.13

## b CO Laser Absorption Diagnostic

A tunable quantum cascade laser was centered at 2059.91 cm<sup>-1</sup> to monitor the P(20) line of the 1 ← 0 transition band of CO. The laser beam is divided into two distinct intensities: the incident intensity  $I_0$  and the transmitted intensity  $I_t$  passing through the reacting gas in the shock tube. Both are collected separately by two InSb detectors after passing a direct-absorption setup. The wavelength was verified before each test with a removable cell containing CO in 90% Ar. Finally, the time-resolved CO mole fractions are calculated using the Beer-Lambert relation, defined as:

$$I_t/I_0 = \exp(-k_\nu PLX_{CO}) \quad (1)$$

where  $k_\nu$  is the absorption coefficient,  $P$  is the partial pressure, and  $L$  is the path length (shock-tube inner diameter), and  $X_{CO}$  the CO mole fraction. The absorption coefficient was calibrated for a large range of temperatures (1180 – 2700 K) at 1 atm and is described as follows:

$$k_\nu = 23.78 \exp^{-0.000646 T} \quad (2)$$

A time-varying absorption coefficient is obtained from numerical predictions of the temperature decrease due to the endothermic decomposition of EC using the Kanayama *et al.* [1] model.

## 3 Results and Discussion

New CO time-history profiles were measured in a heated shock tube for the pyrolysis of EC highly diluted in a mixture of 0.2/0.799 He/Ar. Figure 2 shows representative results at high (1723 K), intermediate (1612 K and 1447 K), and low (1329 K) temperatures. The general feature of each profile shows a nearly linear growth in CO concentration that lasts for a period ranging from a few milliseconds to below 500 microseconds, followed by a period of slower increase in the CO level, corresponding to a transition to a plateau where very little changes in the final CO levels are observed. Typically, the pyrolysis conditions do not permit the CO-to-CO<sub>2</sub> conversion due to the lack of oxygen available in the mixture studied. As one can see, the decrease in the temperature significantly reduces the rate of CO formation, where the coldest temperature of 1329 K does not reach its final CO production level within the time frame of the experiment.

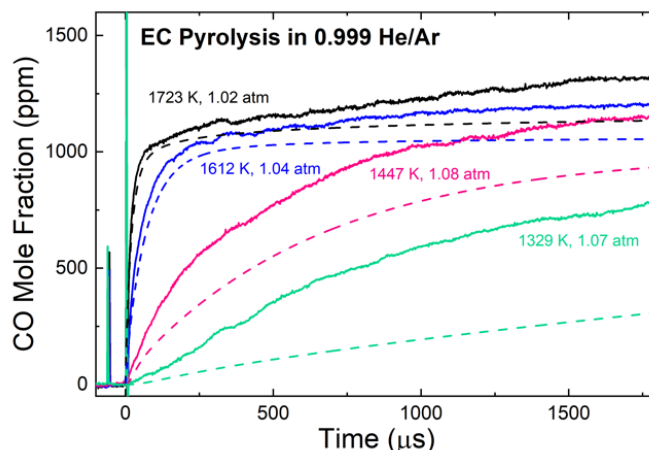
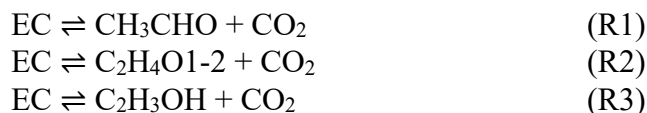


Figure 2: Representative CO time-history profiles for the pyrolysis of EC in 0.2 He/0.799 Ar. The solid lines are the experimental measurements, and the dashed lines represent the predictions from the Kanayama *et al.* [1] model.

Numerical predictions were possible using the Kanayama *et al.* [1] work, where the first EC pyrolysis model available in the literature was proposed. This detailed chemical kinetics mechanism has been developed with *ab initio* theoretical calculations for the thermal decomposition of EC in the gas phase. Dissociation channels were identified (R1-R3), and the reaction R1 was found to be energetically and entropically preferred (67.4 kcal/mol, as opposed to 74.1 kcal/mol, 93.8 kcal/mol for R2 and R3, respectively).



Moreover, the H-atom abstraction reactions with EC (CY(COC\*OOC) in the model), forming CY(CJOC\*OOC), are based on Wildenberg *et al.* [3], by analogy with 1,3-dioxolane. Likewise, additional unimolecular and bimolecular initiation reactions ( $\text{EC} \rightleftharpoons \text{CY}(\text{CJOC}^*\text{OOC}) + \text{H}$  and  $\text{EC} + \text{O}_2 \rightleftharpoons \text{CY}(\text{CJOC}^*\text{OOC}) + \text{HO}_2$ ) are taken into account in the present study to perform numerical predictions for EC oxidation. The subsequent reactions R4 and R5 from CY(CJOC\*OOC) in the literature model are determined with the theoretical calculations.



The comparison of the new CO time histories for EC pyrolysis with the Kanayama *et al.* [1] model in Fig. 2 shows fairly good agreement in the high-temperature range, but major discrepancies are observed for the low-temperature range, where the model underpredicts our profiles by 19.2% and 63.1% at 1500  $\mu\text{s}$  for the temperatures of 1447 K and 1329 K, respectively. A better understanding of EC chemistry is possible using sensitivity and rate-of-production analyses for two distinct temperatures, here 1723 K vs. 1329 K. Figure 3 summarizes the sensitive reactions responsible for the CO formation, where the reactions R1-R2 and R4-R5 play key roles in the EC pyrolysis behavior. From the combination of the sensitivity analysis with the rate-of-production investigation (see Fig. 4), multiple reaction pathways leading to CO can be highlighted:  $\text{EC} \rightarrow \text{CH}_3\text{CHO} \rightarrow \text{CO}$ ,  $\text{EC} \rightarrow \text{C}_2\text{H}_4\text{O1-2} \rightarrow \text{HCO} \rightarrow \text{CO}$ ,  $\text{EC} \rightarrow \text{CY}(\text{CJOC}^*\text{OOC}) \rightarrow \text{CH}_2\text{CHO} \rightarrow \text{CO}$ , and  $\text{EC} \rightarrow \text{CY}(\text{CJOC}^*\text{OOC}) \rightarrow \text{O}^*\text{CCOCJ}^*\text{O} \rightarrow \text{CO}$ .

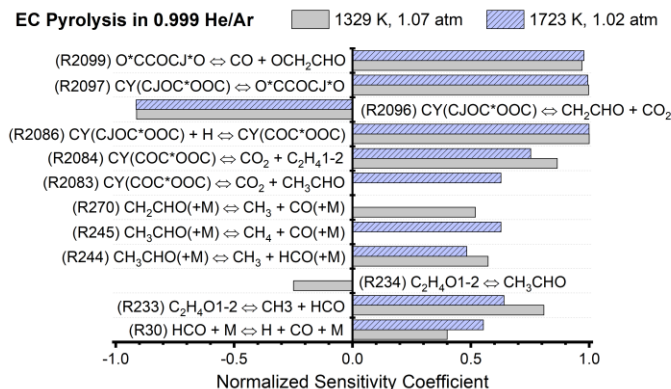


Figure 3: Normalized sensitivity coefficient for CO production during the EC pyrolysis for two representative temperatures at 1329 K, 1.07 atm, and 1723 K, 1.02 atm, respectively.

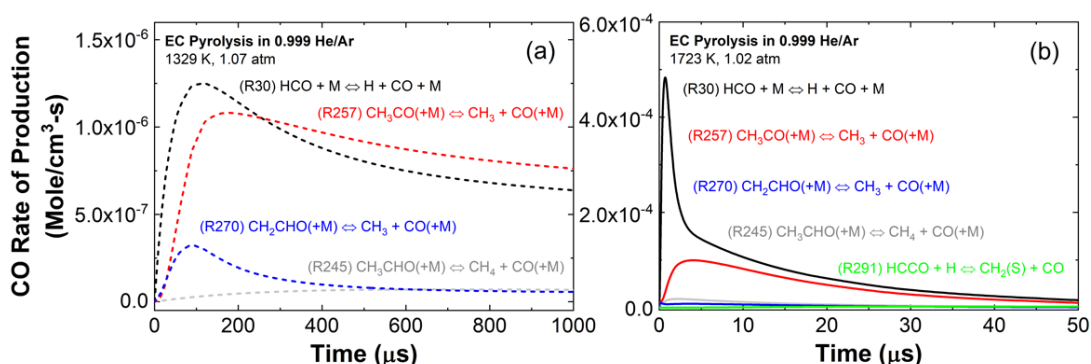


Figure 4: Rate-of-production analysis for CO production during the EC pyrolysis for two representative temperatures at a) 1329 K, 1.07 atm, and b) 1723 K, 1.02 atm, respectively.

Finally, the oxidation of EC behind reflected shock waves was studied to further assess the mechanism. Future work is needed to fully understand the high-temperature chemical kinetics of EC oxidation, as can be seen in Fig. 5. While the CO concentrations decrease after reaching a peak at  $\phi = 0.5$  (CO conversion to the final product  $CO_2$ ), a two-stage induction moment is visible for  $\phi = 1.0$  and 2.0, captured by the numerical predictions from the Kanayama *et al.* [1] model. According to the sensitivity analyses, the second stage is mostly driven by the reaction R6:

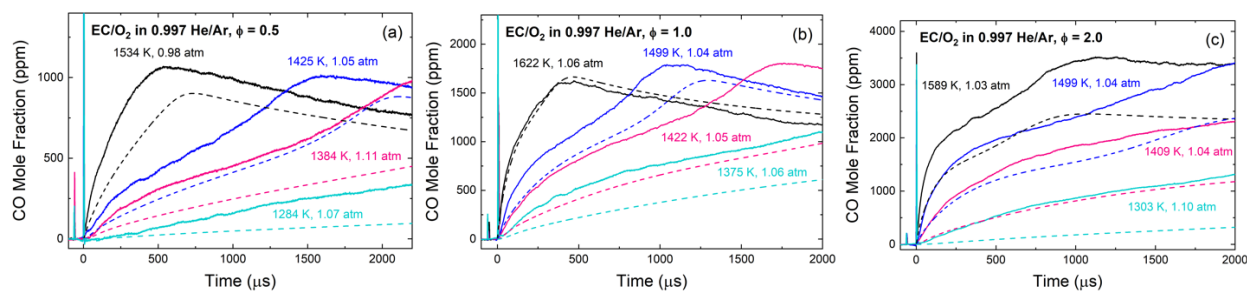
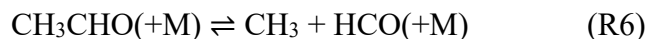


Figure 5: Representative CO time-history profiles for the oxidation of EC in 0.2 He/0.797 Ar at a)  $\phi = 0.5$ , b)  $\phi = 1.0$ , and c)  $\phi = 2.0$ . The solid lines are the experimental measurements, and the dashed lines represent the model.

The mechanism performance at stoichiometric conditions is excellent at 1622 K but is rapidly degraded for lower temperatures. For both the  $\phi = 0.5$  and  $\phi = 2.0$  cases, the detailed mechanism does not reproduce the experimental measurements with great accuracy. While Fig. 6-(a) shows a comparison using CO time-history profiles for the three equivalence ratios at  $\sim 1500$  K and  $\sim 1$  atm, clearly depicting noticeable differences, additional sensitivity analyses are carried out in the same conditions, see Fig. 6-(b). It seems that the reaction R7 inhibits the CO production as a useful H-atom is utilized to form a stable  $\text{CH}_4$  at  $\phi = 2.0$ , whereas the reaction R8 looks less sensitive at  $\phi = 0.5$ , potentially prevented by the short amount of H-atoms in the system.

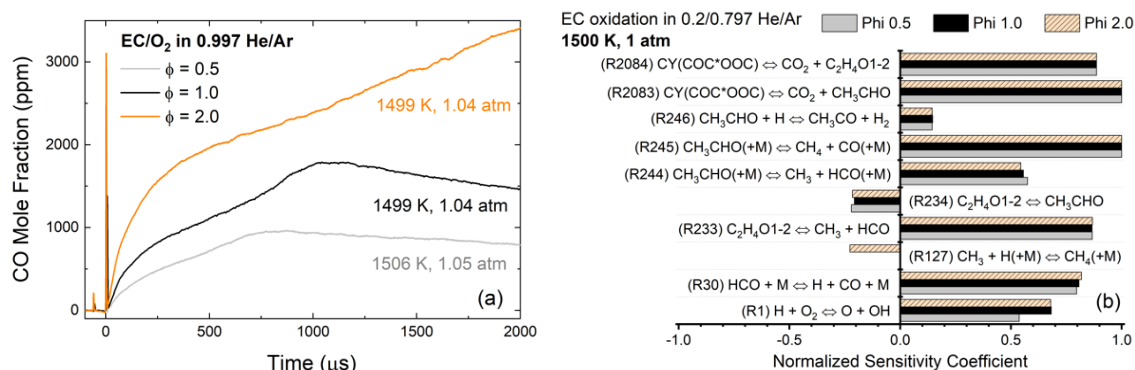


Figure 6: a) CO time histories for three equivalence ratios,  $\phi = 0.5$ , 1.0, and 2.0 at similar conditions. b) CO normalized sensitivity coefficients during the EC oxidation at 1500 K, 1 atm.

## 4 Conclusion

In this study, new CO time-history profiles during EC pyrolysis and oxidation ( $\phi = 0.5$ , 1.0, and 2.0) were measured for temperatures ranging from 1212 to 1734 K, and near-atmospheric pressures behind reflected shock waves in a shock tube at highly diluted conditions (0.997-0.999 He/Ar). The performance of a recent detailed chemical kinetics mechanism from Kanayama *et al.* [1] was evaluated and discrepancies were found. Sensitivity and rate-of-production analyses were performed: many major reactions were emphasized with multiple reactions pathways toward CO being described, such as  $\text{EC} \rightarrow \text{CH}_3\text{CHO} \rightarrow \text{CO}$  and  $\text{EC} \rightarrow \text{C}_2\text{H}_4\text{O1-2} \rightarrow \text{HCO} \rightarrow \text{CO}$ .

## References

- [1] Kanayama K, Takahashi S, Nakamura H, Tezuka T, Maruta K (2022). Experimental and modeling study on pyrolysis of ethylene carbonate/dimethyl carbonate mixture. *Combust. Flame* 245: 112359.
- [2] Mathieu O, Mulvihill C, Petersen EL (2017). Shock-tube water time-histories and ignition delay time measurements for  $\text{H}_2\text{S}$  near atmospheric pressure. *P. Combust. Inst.* 36: 4019.
- [3] Wildenberg A, Fenard Y, Carbonnier M, Kéromnès A, Lefort B, Serinyel Z, Dayma G, Le Moyne L, Dagaut P, Heufer KA (2021). An experimental and kinetic modeling study on the oxidation of 1,3-dioxolane. *P. Combust. Inst.* 38: 543.